Please cite this article in press as: Horn et al., DCC Expression by Neurons Regulates Synaptic Plasticity in the Adult Brain, Cell Reports (2013), http://dx.doi.org/10.1016/j.celrep.2012.12.005

Cell Reports
Article

DCC Expression by Neurons Regulates Synaptic Plasticity in the Adult Brain

Katherine E. Horn,[1] Stephen D. Glasgow,[2] Delphine Gobert,[1] Sarah-Jane Bull,[1] Tamarah Luk,[1] Jacklyn Girgis,[1] Marie-Eve Tremblay,[3] Danielle McEachern,[1] Jean-François Bouchard,[1,6] Michael Haber,[4] Edith Hamel,[1] Paul Krimpenfort,[5] Keith K. Murai,[4] Anton Berns,[5] Guy Doucet,[3] C. Andrew Chapman,[2] Edward S. Ruthazer,[1] and Timothy E. Kennedy[1,*]

[1]Department of Neurology and Neurosurgery, Montreal Neurological Institute, McGill University, Montreal, QC, H3A 2B4, Canada
[2]Center for Studies in Behavioural Neurobiology, Department of Psychology, Concordia University, Montreal, QC, H4B 1R6, Canada
[3]Groupe de Recherche sur le Système Nerveux Central, Département de Pathologie et Biologie Cellulaire, Université de Montréal, Montréal, QC, H3C 3J7, Canada
[4]Centre for Research in Neuroscience, Montreal General Hospital, McGill University, Montreal, QC, H3G 1A4, Canada
[5]Department of Molecular Genetics, Cancer Genomics Centre, Centre for Biomedical Genetics, Netherlands Cancer Institute, Amsterdam, 1066 CX, The Netherlands
[6]Current address: School of Optometry, Université de Montréal, Montreal, Quebec, Canada H3T 1P1
*Correspondence: timothy.kennedy@mcgill.ca
http://dx.doi.org/10.1016/j.celrep.2012.12.005

SUMMARY

The transmembrane protein deleted in colorectal cancer (DCC) and its ligand, netrin-1, regulate synaptogenesis during development, but their function in the mature central nervous system is unknown. Given that DCC promotes cell-cell adhesion, is expressed by neurons, and activates proteins that signal at synapses, we hypothesized that DCC expression by neurons regulates synaptic function and plasticity in the adult brain. We report that DCC is enriched in dendritic spines of pyramidal neurons in wild-type mice, and we demonstrate that selective deletion of DCC from neurons in the adult forebrain results in the loss of long-term potentiation (LTP), intact long-term depression, shorter dendritic spines, and impaired spatial and recognition memory. LTP induction requires Src activation of NMDA receptor (NMDAR) function. DCC deletion severely reduced Src activation. We demonstrate that enhancing NMDAR function or activating Src rescues LTP in the absence of DCC. We conclude that DCC activation of Src is required for NMDAR-dependent LTP and certain forms of learning and memory.

INTRODUCTION

Axon guidance cues are emerging as regulators of synaptogenesis during development; however, their potential contribution to synaptic plasticity in the mature central nervous system (CNS) is not clear (Shen and Cowan, 2010). Here, we asked whether the netrin receptor, deleted in colorectal cancer (DCC), plays a role in synaptic function and plasticity in the adult brain. Many types of neurons express netrin-1 and DCC, and expression is not limited to development. Although both netrin-1 and DCC are essential for normal development, their function in the adult nervous system is not known. Studies in several species support a role for netrins in influencing synaptogenesis during development. Genetic analyses have identified a role for netrin in nerve-muscle synaptogenesis in *Drosophila*. When the amount of netrin expressed by muscle cells is increased, more synaptic connections are made by motoneurons (Mitchell et al., 1996; Winberg et al., 1998), whereas in the absence of DCC, fewer synapses form (Kolodziej et al., 1996). In *Caenorhabditis elegans,* the netrin-1 homolog Unc-6 regulates synaptogenesis by organizing the subcellular distribution of presynaptic proteins (Colón-Ramos et al., 2007; Poon et al., 2008; Stavoe and Colón-Ramos, 2012). In *Xenopus,* application of netrin-1 protein to the optic tectum increases the number of axon branches and synapses made by retinal ganglion cells through a DCC-dependent mechanism (Manitt et al., 2009). The contribution of netrins to synapse formation suggests that DCC expressed by neurons in the mature mammalian brain may influence synapse function and plasticity. Notably, DCC activates the cytoplasmic tyrosine kinase Src in neurons (Li et al., 2004). Activation of Src regulates NMDA receptor (NMDAR) function and is essential for long-term potentiation (LTP), a form of activity-dependent synaptic plasticity (Lu et al., 1998). Here, we tested the hypothesis that DCC expressed by neurons regulates synaptic plasticity in the adult brain.

RESULTS

DCC Enrichment at Synapses

To establish whether netrin-1 and DCC are present at synapses in the mature mammalian brain, we fractionated subcellular components of adult rat hippocampus (Huttner et al., 1983). We found that both netrin-1 and DCC are present in synaptosomes (fraction P2, Figure 1A). Following synaptosome lysis and further fractionation, netrin-1 and DCC were present in fraction LP1, which is composed of pre- and postsynaptic

Please cite this article in press as: Horn et al., DCC Expression by Neurons Regulates Synaptic Plasticity in the Adult Brain, Cell Reports (2013), http://dx.doi.org/10.1016/j.celrep.2012.12.005

Cell PRESS
Open ACCESS

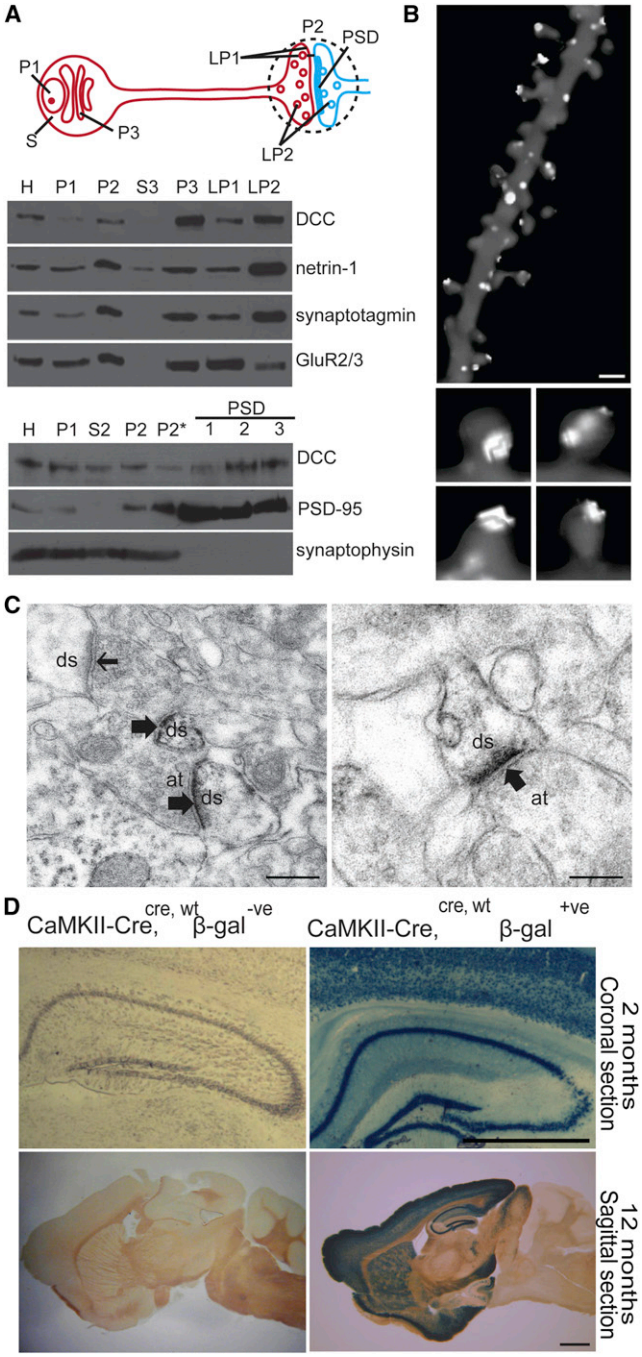

Figure 1. DCC Is Enriched in Mature Dendritic Spines

(A) Subcellular fractionation of adult rat brain. The diagram illustrates fractions of interest. DCC and netrin-1 are present in synaptic fractions, and DCC enriches with the PSD. H, whole-brain homogenate; P1, pellet with nuclear and cellular debris; P2, mitochondria and synaptosome-enriched pellet; S2 and S3, soluble fractions; P2*, synaptosome-enriched pellet; LP1, synaptic plasma membrane enriched; LP2, synaptic vesicle enriched.

(B) DCC immunoreactivity (white) on dendritic spines along an fRFP-labeled dendrite. Scale bar, 1 μm. Enlarged images of DCC-immunoreactive spines are shown below.

(C) Immunoelectron microscopy detects DCC immunostaining at PSDs of a subset of dendritic spines (wide arrows) but not at others (narrow arrow). Scale bars, left: 0.5 μm; right: 0.25 μm. at, axon terminal; ds, dendritic spine.

(D) *Cre* is broadly expressed in the forebrain in progeny of T29-1 CaMKIIα-Cre crossed with ROSA26-lacZ mice. Brain sections were obtained from β-gal-negative (left) and -positive (right) 2- and 12-month-old mice (β-gal stain). Neuronal expression of *cre* was observed in CA1, CA3, the dentate gyrus, and the neocortex in coronal (top) and sagittal (bottom) sections. Scale bar, 1 mm.

plasma membranes, consistent with enrichment of GluA2/3 in this fraction. DCC and netrin-1 were also enriched in fraction LP2, which contains synaptotagmin- and synaptophysin-positive transmitter vesicles and various cargo transport vesicles. Fractionation of adult rat brain to enrich for the postsynaptic density (PSD) (Fallon et al., 2002) revealed DCC cofractionating with the PSD protein PSD-95 (Figure 1A). These results provide evidence that netrin-1 and DCC are enriched at mature synapses associated with synaptic plasma membranes and intracellular vesicles, and that DCC cofractionates with the PSD.

Dendritic spines are postsynaptic specializations that undergo activity-dependent changes in shape and number that are thought to be important for learning and memory (Nimchinsky et al., 2002). To examine the distribution of DCC in CA1 pyramidal cell dendrites and spines, we imaged hippocampal organotypic slices infected with a Semliki Forest virus encoding membrane-targeted farnesylated red fluorescent protein (fRFP) (Haber et al., 2006). The results demonstrated a striking enrichment of DCC immunoreactivity in the head of dendritic spines (Figure 1B). Consistent with this distribution, immunoelectron microscopy revealed enrichment of DCC in PSDs in the CA1 stratum radiatum of adult rat brain (Figure 1C). These findings demonstrate that DCC is enriched at mature synapses in dendritic spines.

Conditional Deletion of *DCC* from Forebrain Neurons

DCC is expressed by dentate gyrus granule cell neurons, hippocampal CA1 and CA3 pyramidal neurons, and neurons throughout the neocortex during postnatal development and in adults (Livesey and Hunt, 1997; Volenec et al., 1997). Conventional *DCC* null mice die within hours of birth, which makes it impossible to examine synaptic plasticity in the adult CNS in these animals (Fazeli et al., 1997; Serafini et al., 1996). To delete *DCC* selectively from neurons in the mature brain, we adopted a cre/loxP gene-targeting strategy (Sauer, 1998). Floxed *DCC* (*DCC*$^{f/f}$) mice were crossed to a line expressing *cre* regulated by the promoter of the α-subunit of the Ca^{2+}/calmodulin-dependent kinase II gene (T29-1 *CaMKIIα-cre*), which drives expression exclusively by neurons in the adult forebrain (Benson et al., 1992; Burgin et al., 1990; Jacobs et al., 1993). Although endogenous CaMKIIα is not expressed during embryogenesis, upregulation occurs postnatally (Bayer et al., 1999). Critically, *cre* is expressed by neurons after axon guidance is complete, which gives us the opportunity to selectively address DCC function in mature neural circuits in vivo.

Cre is first expressed in T29-1 *CaMKIIα-cre* mice at ~2.5 weeks of age and is initially restricted to CA1 hippocampal pyramidal neurons (Tsien et al., 1996). By 1 month of age (Sonner et al., 2005), *cre* is expressed by CA1 and CA3 pyramidal neurons, dentate gyrus granule cells, and neurons throughout

Please cite this article in press as: Horn et al., DCC Expression by Neurons Regulates Synaptic Plasticity in the Adult Brain, Cell Reports (2013), http://dx.doi.org/10.1016/j.celrep.2012.12.005

the neocortex, but not by glia. We confirmed this pattern of expression by crossing T29-1 mice with *ROSA26-lacZ* reporter mice (Soriano, 1999), which express β-galactosidase (β-gal) following *cre*-induced recombination (Figure 1D). Crossing the $DCC^{f/f}$ mice with T29-1 mice generated conditional *DCC* knockouts ($DCC^{f/f,cre+}$) that are homozygous $DCC^{f/f}$ and carry at least one copy of *CaMKIIα-cre*. The crosses also yield $DCC^{f/f,wt/wt}$ and $DCC^{f/wt,wt/wt}$ littermates that were used as wild-type (WT) controls. All analyses used male mice only.

Levels of DCC protein in the hippocampus of $DCC^{f/f,cre+}$ mice were substantially reduced at 3, 8, and 18 months of age (Figures 2A and 2B) but were unchanged at postnatal day 14 (P14) (Figure 2A), indicating that normal levels of DCC are present throughout embryogenesis and initial maturation of the nervous system. Conventional DCC knockouts lack a corpus callosum (Fazeli et al., 1997). Cresyl violet staining revealed no obvious gross morphological changes in the brains of adult $DCC^{f/f,cre+}$ mice (Figure 2C), which is consistent with normal expression of DCC in young mice and demonstrates the feasibility of removing DCC from neurons after axon guidance is complete.

We previously reported defects in axo-oligodendroglial paranodal junctions in conventional *DCC* knockout mice that result from the absence of DCC function in oligodendrocytes (Jarjour et al., 2008). No such deficit was found in the hippocampi of adult $DCC^{f/f,cre+}$ mice, in which *DCC* is deleted only from neurons (Figure 2D). Consistent with selective deletion of DCC from neurons, immunohistochemical staining for cre and the astrocyte marker glial fibrillary acidic protein (GFAP) did not label the same cells (Figure 2E, top panels). We also assessed the distribution of cells expressing *cre* using β-gal expression in the progeny of T29-1 mice crossed with *ROSA26-lacZ* reporter mice. β-gal, indicating *cre* expression, did not overlap with tyrosine hydroxylase (TH)-immunopositive neurons, consistent with *cre* not being expressed by ventral midbrain dopaminergic neurons (Figure 2E, bottom panels).

In 2- to 4-month-old mice (hereafter referred to as young adults) and 5-month-old and older mice (hereafter referred to as older adults), although the levels of DCC in hippocampal homogenates were significantly decreased, we did not detect significant changes in the expression of a variety of synaptic proteins (Figure 2F).

DCC-Deficient Dendritic Spines Are Smaller

To determine whether DCC influences dendritic spine morphology, we first established hippocampal organotypic slice cultures derived from conventional *DCC* knockout mice (Fazeli et al., 1997). Adult *DCC* heterozygotes were crossed to generate litters composed of newborn *DCC* null pups (Fazeli et al., 1997), heterozygotes, and WT littermate controls. To visualize dendrites, hippocampal cultures derived from null and WT pups were infected with Semliki Forest virus encoding membrane-targeted green fluorescent protein (GFP) (Haber et al., 2006). Analysis of dendritic spine morphology in pyramidal neurons that had never expressed DCC revealed significantly smaller spines (Figure 3A), with reduced spine head size and neck width, compared with controls (Figure 3B).

To determine whether selective postnatal deletion of *DCC* from neurons would alter dendritic spine morphology in vivo, we examined the brains of young (2–4 months) and older (>5 months) $DCC^{f/f,cre+}$ and age-matched controls using the Golgi-Cox staining technique (Figure 3C). Spines were quantified along segments of dendrites of CA1 hippocampal neurons (Figure 3A) by an investigator blind to genotype. No significant difference was found in spine density or head width, but a significant decrease in spine length was detected along dendritic branches in older $DCC^{f/f,cre+}$ mice compared with control mice (Figure 3D). Importantly, no significant difference was detected in the younger mice, indicating that the loss of *DCC* expression by mature neurons in the $DCC^{f/f,cre+}$ mice results in a decrease in spine size as the mice age.

DCC Loss Impairs Memory

To test the hypothesis that DCC contributes to memory, we used the Morris water maze, a hippocampus-dependent spatial memory task (Clark and Martin, 2005). For 3 days, mice were trained to swim to a visible platform. All of the mice performed comparably and reached the platform within the same time on the third day, indicating intact sensory and motor function. After training, the spatial visual cues in the surroundings were switched and the mice learned anew to swim to a submerged platform located in a different quadrant of the maze. On the eighth day, 2 hr after the last test, the platform was removed, and a probe trial was run in which the time and distance spent in the appropriate quadrant were measured. Testing young $DCC^{f/f,cre+}$ and littermate control mice (2–4 months old) revealed no significant difference between groups (Figures 4A–4C). However, when the same mice were tested using this 8 day protocol at >5 months of age, the probe trial revealed that the control mice traveled significantly farther and spent more time in the appropriate quadrant than their $DCC^{f/f,cre+}$ counterparts, and made more passes over the former location of the submerged platform (Figures 4D–4F). Swimming speed did not vary between genotypes at any age (Figures 4A and 4D). These findings identify a spatial memory impairment in older $DCC^{f/f,cre+}$ mice.

We also applied the novel-object-recognition test, which is based on the tendency of normal mice to interact more with novel objects than with familiar objects (Bevins and Besheer, 2006). In this test, each mouse is first habituated to an empty field, and the next day the mouse is returned to the same open field, now containing two identical, biologically neutral objects, which it is allowed to explore for 5 min. After a 4 hr rest, the mouse is returned to the open field, where one familiar object has been replaced by a novel object (Figure 4G). The relative amount of time spent attending to the novel object can be used as a measure of the memory for the familiar object (Bevins and Besheer, 2006). We then calculated cognition and difference scores for 24 $DCC^{f/f,cre+}$ mice and 24 controls, with the experimenter being blind to genotype. The total time spent exploring the two objects did not differ between genotypes (Figure 4H); however, novel-object recognition was significantly impaired in $DCC^{f/f,cre+}$ mice (Figures 4I and 4J). When performance was binned based on age, young (2–4 months) $DCC^{f/f,cre+}$ mice were not different from controls, whereas older (>5 months) $DCC^{f/f,cre+}$ mice were significantly impaired in recognition memory compared with age-matched controls (Figures 4I and 4J).

Please cite this article in press as: Horn et al., DCC Expression by Neurons Regulates Synaptic Plasticity in the Adult Brain, Cell Reports (2013), http://dx.doi.org/10.1016/j.celrep.2012.12.005

Cell PRESS
Open ACCESS

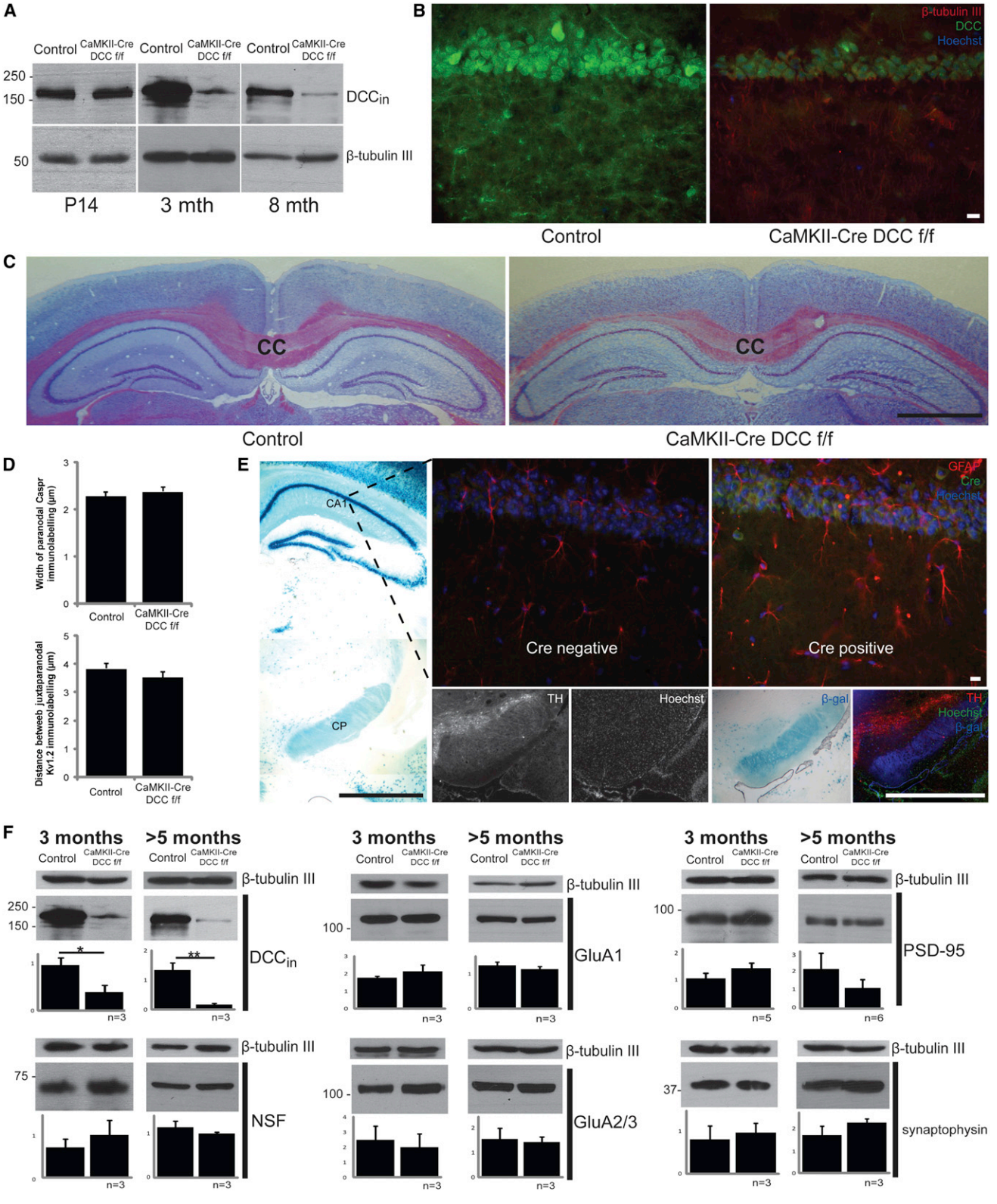

Figure 2. Characterization of DCC$^{f/f,cre+}$ Mice

(A) Western blots of hippocampal homogenates from P14, 3-month-old, and 8-month-old controls and DCC$^{f/f,cre+}$ littermates show decreased levels of DCC in adult DCC$^{f/f,cre+}$ mice.

(legend continued on next page)

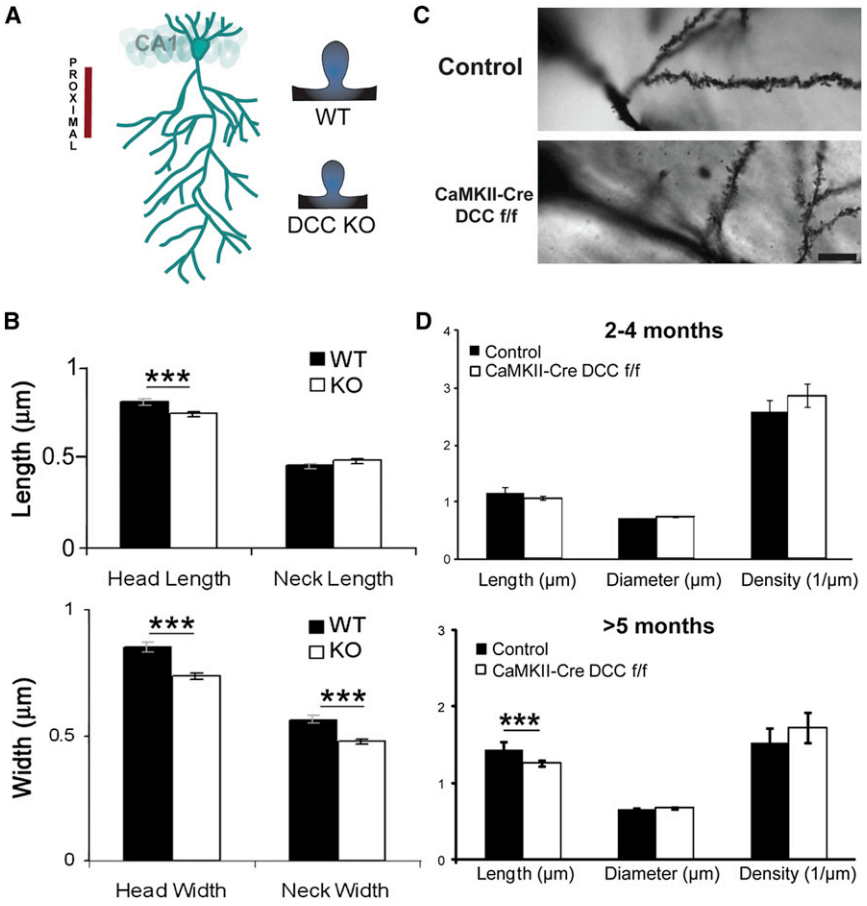

Figure 3. DCC Deficiency Decreases Spine Size

(A) Illustration of CA1 pyramidal neuron dendritic branching and spine morphology of DCC-deficient mice.

(B) Hippocampal organotypic slice cultures from P0 conventional DCC knockout or WT pups were infected with a virus encoding farnesylated GFP (fGFP). Analysis revealed decreased spine head length and width and neck width in DCC null neurons (***$p < 0.005$; error bars depict SEM).

(C) Representative images of Golgi-Cox stained spines from control and $DCC^{f/f,cre+}$ mice. Scale bar, 10 μm.

(D) Analysis of Golgi-Cox stained spines of young (2–4 months) and older (>5 months) mice. Spines from proximal CA1 pyramidal dendritic branches in older $DCC^{f/f,cre+}$ mice exhibit significantly reduced spine length (***$p < 0.005$; error bars depict SEM).

Importantly, the behavioral tests revealed no significant difference between the young $DCC^{f/f,cre+}$ and control mice. We conclude that deficits develop during aging as a result of the absence of DCC function in neurons, and that DCC expression by neurons in the mature brain contributes to spatial memory and the recognition of novelty.

Impaired LTP but not Long-Term Depression in DCC-Deficient Mice

To determine whether DCC loss leads to changes in synaptic efficacy, we used acute hippocampal slices from both young (2–4 months) and older (>5 months) adult $DCC^{f/f,cre+}$ or age-matched control mice to record field excitatory postsynaptic potentials (fEPSPs) in CA1 evoked by stimulation of the Schaffer collaterals. Analysis of the input/output relationship at CA3-CA1 synapses across a range of stimulus intensities did not detect significant differences between hippocampal slices derived from older $DCC^{f/f,cre+}$ and control mice (Figure 5A). Critically, this indicates that CA3-CA1 synaptic contacts are intact in animals lacking DCC, and that basal levels of synaptic transmission in $DCC^{f/f,cre+}$ mice are not altered by the deletion of DCC. To determine whether DCC deletion influences synaptic plasticity, we next assessed LTP and long-term depression (LTD) at CA3-CA1 Schaffer collateral synapses (Figure 5).

LTP is an experimental model of activity-dependent synaptic strengthening that may function as a neural substrate underlying learning and memory (Bliss and Collingridge, 1993). To assess the role of DCC in LTP, we used high-frequency stimulation (HFS; 1 s, 100 Hz) to induce LTP in hippocampal slices derived from $DCC^{f/f,cre+}$ mice and age-matched controls (Figures 5B and 5C). Whereas slices from control animals showed robust LTP, slices from older (>5 months) $DCC^{f/f,cre+}$ mice exhibited a striking absence of potentiation 1 hr after induction (Figure 5B). To determine whether this impairment was due to a developmental deficit in $DCC^{f/f,cre+}$ animals, we tested hippocampal

(B) Immunostained CA1 in hippocampal sections from 18-month-old control and $DCC^{f/f,cre+}$ mice (red, β-tubulin III; green, DCC; blue, Hoechst; scale bar, 10 μm).

(C) Cresyl-violet-stained coronal sections of 18-month-old control and $DCC^{f/f,cre+}$ mice. Scale bar, 1 mm. CC, corpus callosum.

(D) Axo-oligodendroglial paranodes of 8-month-old control and $DCC^{f/f,cre+}$ mice exhibit no significant differences in width of Caspr immunoreactivity or distance between Kv1.2 juxtaparanodes. Error bars depict SEM.

(E) Immunohistochemical staining of cre-positive and -negative coronal brain sections. A section from cre-positive progeny of T29-1 CaMKIIα-Cre crossed with ROSA26-lacZ mice (far left) shows the location of immunostained regions (scale bar, 1 mm). Top panels show hippocampal CA1 from cre-positive and -negative mice (red, GFAP; green, Cre; blue, Hoechst; scale bar, 10 μm). Bottom panels show adjacent brain sections containing substantial nigra (TH-positive) of cre-positive progeny. An overlay of stained sections is shown in the far-right bottom panel (red, TH; green, Hoechst; blue, β-gal; scale bar, 1 mm).

(F) Western blots of hippocampal homogenates of young (3 months) and older (>5 months) mice. Histograms plot the average intensity from control and $DCC^{f/f,cre+}$ mice (n/genotype indicated under histogram) normalized using β-tubulin III as a loading control (Student's two-tailed t test, *$p < 0.05$, **$p < 0.01$; error bars depict SEM).

Please cite this article in press as: Horn et al., DCC Expression by Neurons Regulates Synaptic Plasticity in the Adult Brain, Cell Reports (2013), http://dx.doi.org/10.1016/j.celrep.2012.12.005

Cell PRESS
Open ACCESS

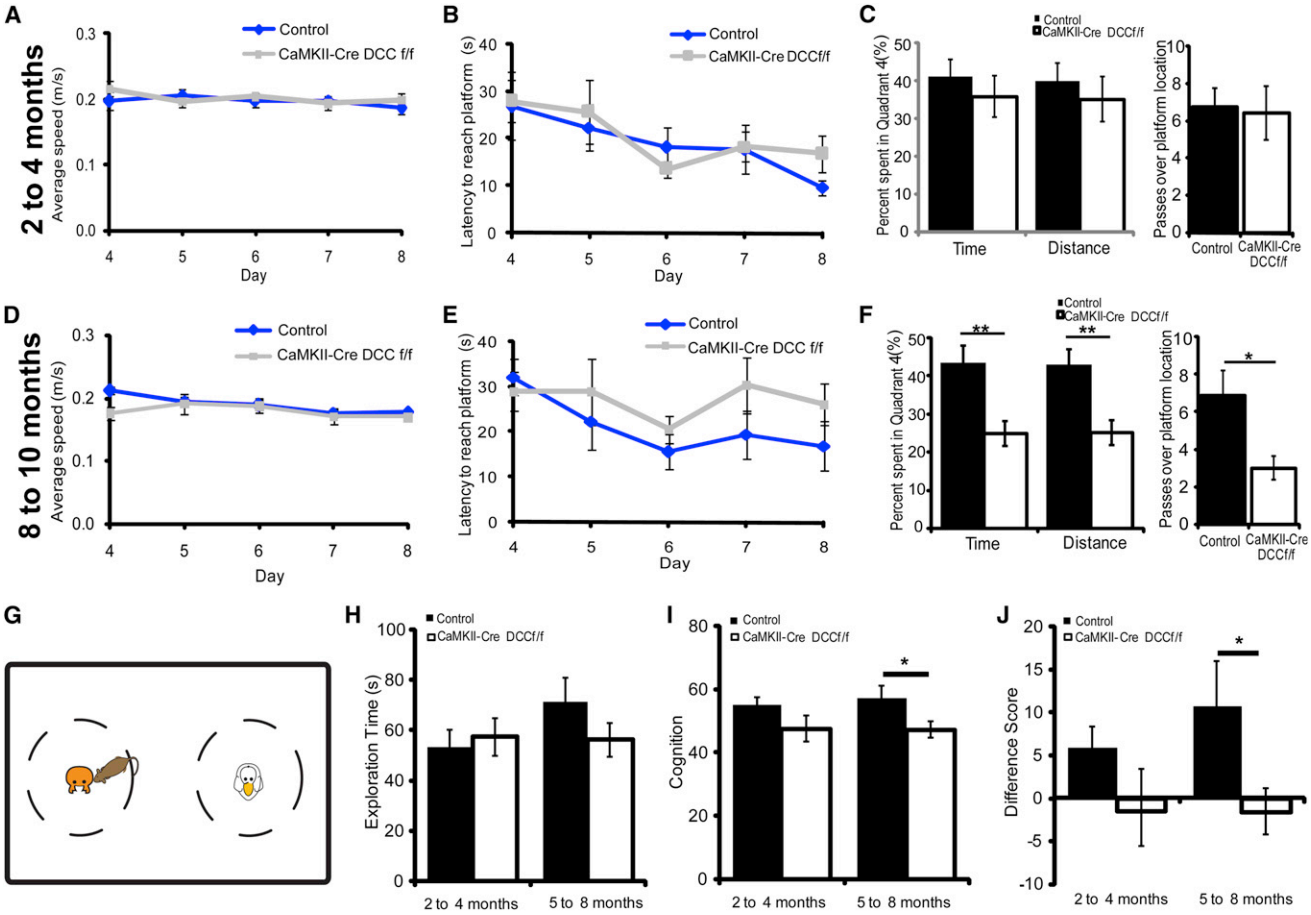

Figure 4. Impaired Spatial and Recognition Memory in Aged *DCC*$^{f/f,cre+}$ Mice

(A–F) Morris water maze. Young (A) and older (D) controls and *DCC*$^{f/f,cre+}$ mice swim at similar speeds. Genotypes show no difference between young (B) and older (E) mice during training to learn the location of a submerged platform. In a probe trial to test spatial memory of the location of the submerged platform, 2 hr after the last day of training, passes over the former location of the platform, distance, and time in the appropriate quadrant were analyzed (C and F). Young (2–4 months) control and *DCC*$^{f/f,cre+}$ mice perform similarly (n = 8/group) (C). (F) Older (>5 months) *DCC*$^{f/f,cre+}$ mice score lower than controls (control: n = 7, *DCC*$^{f/f,cre+}$: n = 8). Statistical analysis was performed using a two-tailed t test (*$p < 0.05$, **$p < 0.01$; error bars depict SEM).

(G) Diagram of the novel-object-recognition test.

(H) Young (2–4 months) and older (>5 months) control and *DCC*$^{f/f,cre+}$ mice explore objects for similar durations (young control: n = 13; young *DCC*$^{f/f,cre+}$: n = 11, older control: n = 11; older *DCC*$^{f/f,cre+}$: n = 13).

(I and J) Performance was worse for older *DCC*$^{f/f,cre+}$ mice in cognition (I) and difference (J) scores (two-tailed t test; *$p < 0.05$; error bars depict SEM).

slices from 2- to 4-month-old *DCC*$^{f/f,cre+}$ mice (Figure 5C). In contrast to their aged counterparts, fEPSPs in slices from young (2–4 months) *DCC*$^{f/f,cre+}$ mice and their age-matched controls demonstrated significant potentiation 1 hr post-tetanus (*DCC*$^{f/f,cre+}$ versus age-matched controls, $p > 0.05$). We conclude that the impairment exhibited by older animals is not due to a deficit in the early development of *DCC*$^{f/f,cre+}$ mice. We also assessed fEPSP amplitudes during the HFS train and found no significant differences between genotypes (Figure 5D), suggesting that the lack of LTP did not resulting from an inability to follow the HFS train.

To determine whether LTP impairment may be due to altered presynaptic function, we examined paired-pulse facilitation (PPF) across a range of stimulus intervals. Changes in PPF are generally attributed to changes in the probability of presynaptic transmitter release. PPF ratios were not significantly different in slices from older (>5 months) control and *DCC*$^{f/f,cre+}$ mice at intervals ranging from 20 to 100 ms (Figure 5E), or in slices from younger control and *DCC*$^{f/f,cre+}$ mice (data not shown). The absence of a difference in PPF supports the conclusion that deletion of DCC does not result in a significant alteration in presynaptic transmitter release, and is consistent with DCC deletion resulting in a postsynaptic deficit.

Repeated low-frequency stimulation (LFS) induces LTD of evoked responses at CA3-CA1 synapses. To determine whether DCC contributes to LTD, we used a paired-pulse LFS (PPLFS) paradigm to induce LTD (15 min, 1 Hz paired-pulse stimulation, 1,800 pulses, 25 ms interpulse interval; Kourrich et al., 2008). Hippocampal slices from >5 months old *DCC*$^{f/f,cre+}$ mice and their age-matched controls demonstrated significant depression

Please cite this article in press as: Horn et al., DCC Expression by Neurons Regulates Synaptic Plasticity in the Adult Brain, Cell Reports (2013), http://dx.doi.org/10.1016/j.celrep.2012.12.005

Cell PRESS
Open ACCESS

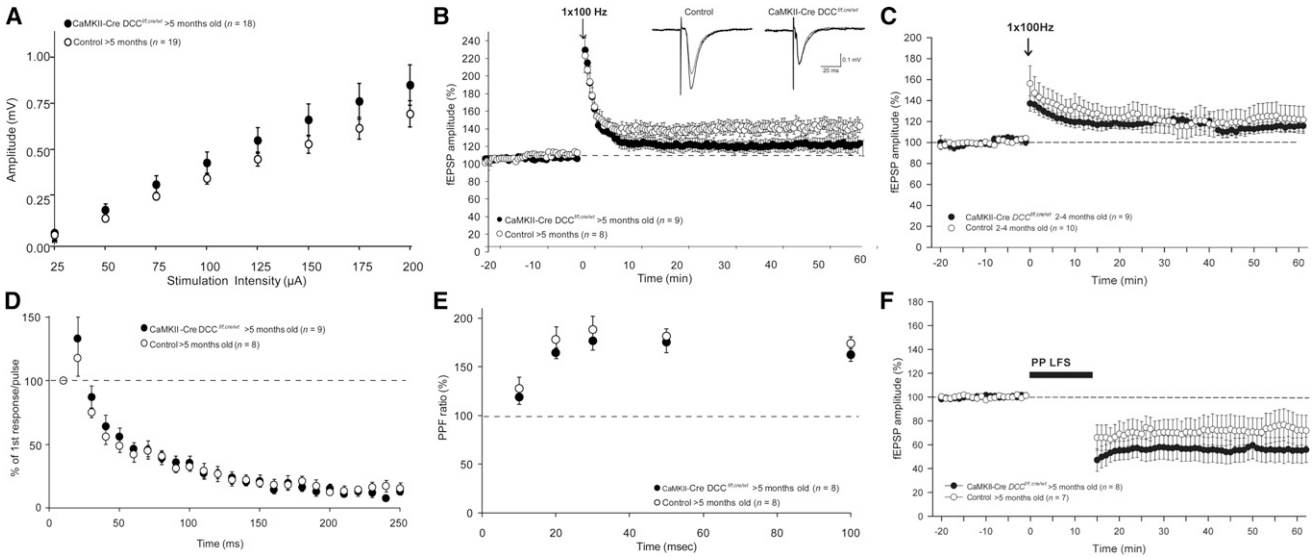

Figure 5. Impaired LTP but Intact LTD in *DCC*$^{f/f,cre+}$ Mice

(A) No significant difference is detected between control and *DCC*$^{f/f,cre+}$ in CA3-CA1-evoked fEPSP amplitudes in older animals.

(B) Following HFS in older animals (>5 months), DCC$^{f/f,cre+}$ does not display LTP. The mean amplitude of fEPSPs is potentiated in control (137.6% ± 8.0%, $p < 0.001$) but not in DCC$^{f/f,cre+}$ slices at 1 hr (116.1% ± 8.2%; $p > 0.05$). Representative fEPSPs from control (left) and DCC$^{f/f,cre+}$ (right) before (gray) and after (black) HFS (arrow) are shown.

(C) Slices from young (2–4 months) *DCC*$^{f/f,cre+}$ mice and age-matched controls remain significantly potentiated 1 hr after HFS (113.9% ± 5.2% in *DCC*$^{f/f,cre+}$ versus 121.3% ± 12.5% in controls, $p > 0.05$).

(D) No significant differences in fEPSP amplitude during the HFS train between older (>5 months) control and *DCC*$^{f/f,cre+}$ mice are observed.

(E) PPF ratios in slices from older control and *DCC*$^{f/f,cre+}$ mice do not differ significantly ($p > 0.05$).

(F) PPLFS (bar, 15 min) induced LTD in older control (n = 7) and DCC$^{f/f,cre+}$ mice (n = 8; $p < 0.01$ versus baseline).

of synaptic responses following PPLFS ($p < 0.01$; Figure 5F), indicating that the LTP deficit is the not the result of a general loss of synaptic plasticity.

DCC Regulates NMDAR Subunit GluN2B Expression

We then investigated the mechanism that underlies the deficit in LTP induction in *DCC*$^{f/f,cre+}$ mice. Western blot analyses revealed no significant change in the expression of the synaptic proteins synaptophysin, N-ethylmaleimide-sensitive factor (NSF), AMPA receptor (AMPAR) subunits GluA1 and GluA2/3, or NMDAR subunits GluN1 and GluN2A in hippocampal homogenates of adult *DCC*$^{f/f,cre+}$ mice compared with controls (Figures 2F and 6A). In contrast, a significant increase in the amount of NMDAR subunit GluN2B was found in young (3 months) and older (>5 months) *DCC*$^{f/f,cre+}$ mice (Figure 6A) that persisted in 20-month-old *DCC*$^{f/f,cre+}$ mice (Figure 6B). Increased GluN2B protein was detected in whole hippocampal homogenates and in the synaptosome LP1 plasma membrane fraction (Figure 6B), which includes the synaptic apposition and extrasynaptic plasma membranes.

To determine whether increased levels of GluN2B contribute to electrophysiological differences in slices from control and *DCC*$^{f/f,cre+}$ mice, we examined the various currents that contribute to the fEPSP response in slices from older (>5 months) control and *DCC*$^{f/f,cre+}$ mice by applying appropriate pharmacological inhibitors (Figure 6C). Following application of picrotoxin (PTX) and 6-cyano-7-nitroquinoxaline-2,3-dione (CNQX) to block GABA receptors and AMPARs, respectively, we added ifenprodil to selectively block the function of GluN2B-contaning NMDARs. In the presence of ifenprodil, we observed no difference in the evoked NMDAR-mediated responses between *DCC*$^{f/f,cre+}$ mice and their age-matched controls (Figure 6D). This result indicates that the increased expression of GluN2B in *DCC*$^{f/f,cre+}$ mice does not alter the electrophysiological response, which suggests that the increased GluN2B protein is not located at synapses.

DCC Regulates Src, Phospholipase C γ, and Phosphorylated Src Family Kinase Expression

DCC activates both phospholipase C (PLC) and Src family kinases (SFKs) in neurons (Liu et al., 2004; Xie et al., 2006), and activation of the tyrosine kinase Src is necessary and sufficient for the induction of LTP (Lu et al., 1998). Src regulates NMDAR function by phosphorylating the GluN2A subunit (Salter and Kalia, 2004), and PLC activation of Src through protein kinase C (PKC) increases the opening probability and open time of NMDAR without changing the channel conductance or reversal potential (MacDonald et al., 2007; Yu et al., 1997; Yu and Salter, 1998). We therefore investigated how loss of DCC might alter the expression and function of these proteins.

In hippocampal homogenates of older (>5 months), but not young (3 months) *DCC*$^{f/f,cre+}$ mice, we detected a significant decrease in the amount of phosphorylated PLCγ1, but not total PLCγ1 (Figure 7A), consistent with reduced PLCγ1 activation in the absence of DCC. We also identified a significant decrease in the amount of total Src protein in the *DCC*$^{f/f,cre+}$ animals, but no

Please cite this article in press as: Horn et al., DCC Expression by Neurons Regulates Synaptic Plasticity in the Adult Brain, Cell Reports (2013), http://dx.doi.org/10.1016/j.celrep.2012.12.005

Cell PRESS
Open ACCESS

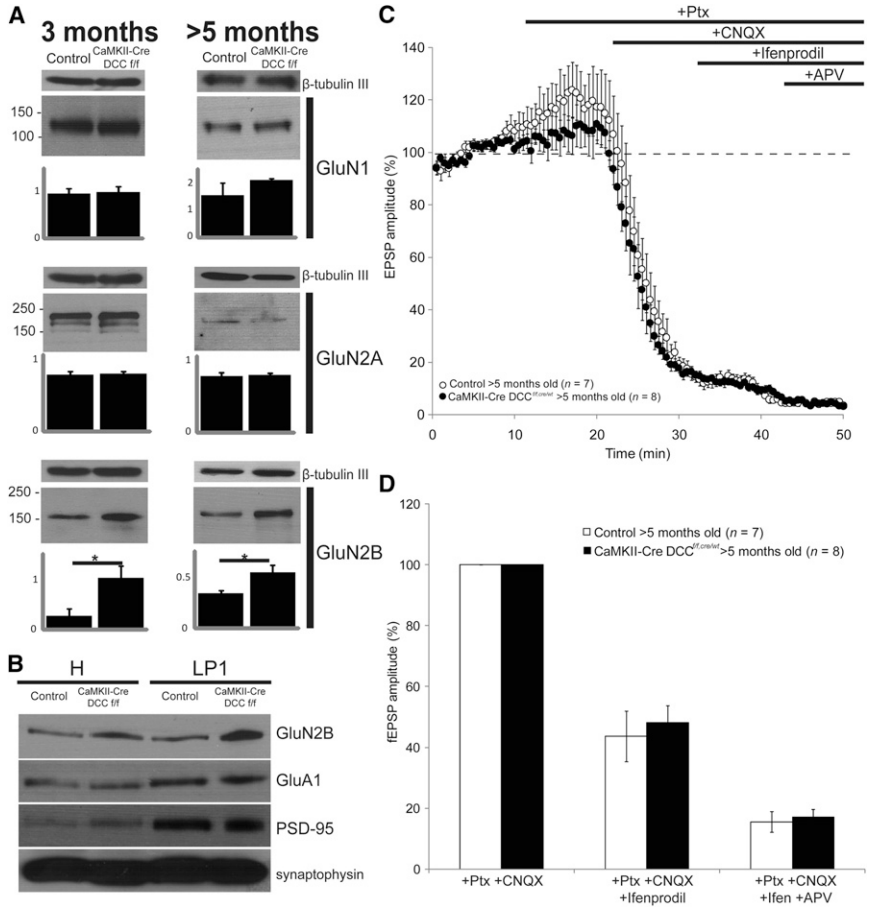

Figure 6. DCC Regulates NMDAR Function

(A) Protein expression levels of NMDAR subunits in hippocampal homogenates from young (3 months) and older (>5 months) mice (n = 3/genotype; two-tailed t test, *p < 0.05; error bars depict SEM).

(B) Subcellular fractionation of hippocampi from control and $DCC^{f/f,cre+}$ mice (20 months old). In $DCC^{f/f,cre+}$ mice, GluN2B is enriched in the LP1 synaptic membrane fraction. No significant changes were detected between genotypes in levels of GluA1, PSD-95, or synaptophysin.

(C) Pharmacological inhibitors were applied to slices of older (>5 months) control and $DCC^{f/f,cre+}$ mice in low-Mg^{2+} (0.1 mM) ACSF. fEPSP amplitude was measured during this treatment.

(D) No significant difference was detected in fEPSP amplitudes measured for control and $DCC^{f/f,cre+}$ mice. Normalized fEPSP amplitude in the presence of PTX and CNQX is shown; error bars depict SEM.

change in the SFK Fyn. Furthermore, we detected decreased pan-SFK Y416 phosphorylation, revealing substantially reduced SFK activity in neurons lacking DCC (Figure 7A). Activation of DCC by addition of netrin-1 to synaptosomes purified from the cortex of WT adult mice increased phosphorylated SFK (pSFK) compared with unstimulated control synaptosomes (Figure 7B), providing evidence that netrin-1 activates SFKs at synapses. The emergence of these deficits with age supports the conclusion that loss of DCC results in a deficit in key synaptic signaling mechanisms in older adults.

The influx of calcium (Ca^{2+}) through NMDARs is critical for the induction of LTP, but is blocked by magnesium (Mg^{2+}) at resting membrane potentials. SFK activation promotes the influx of Ca^{2+} through the NMDAR by increasing both the probability of NMDAR opening and the open time (Lu et al., 1998; Salter and Kalia, 2004; Yu and Salter, 1998). To determine whether the LTP deficit in older (>5 months) $DCC^{f/f,cre+}$ mice is a consequence of reduced Ca^{2+} influx through NMDARs, we facilitated NMDAR function by reducing the concentration of Mg^{2+} from 2.0 mM to 1.3 mM in the artificial cerebrospinal fluid (ACSF) perfusing the slice. This resulted in a striking rescue of LTP following HFS (1 s, 100 Hz) in hippocampal slices derived from older (>5 months) $DCC^{f/f,cre+}$ mice, resulting in LTP that was indistinguishable from that evoked in age-matched controls in the same ACSF (Figure 7C).

We then directly tested the hypothesis that the LTP deficit in older (>5 months) $DCC^{f/f,cre+}$ mice is specifically due the lack of activated Src. We thus aimed to selectively activate Src in the $DCC^{f/f,cre+}$ mice and determine whether this was sufficient to rescue LTP in the absence of DCC. To do this, we applied pituitary adenylate cyclase activating peptide-38 (PACAP-38), a 38 amino acid peptide that activates PAC_1R, a G-protein-coupled receptor expressed by hippocampal neurons (Miyata et al., 1990; Zhou et al., 2000). PACAP-38 binding of PAC_1R signals through PLC and PKC to activate Src and enhance NMDAR function (Macdonald et al., 2005). Application of PACAP-38 during the HFS train (1 s, 100 Hz) rescued LTP in hippocampal slices derived from older (>5 months) $DCC^{f/f,cre+}$ mice in ACSF containing 2.0 mM of Mg^{2+}. Critically, this rescue was blocked by addition of the SFK inhibitor PP2 but not its inactive analog, PP3 (Figure 7D), indicating that SFK activation was essential for PACAP-38 to rescue LTP. We conclude that in the absence of DCC, substantially reduced SFK signaling underlies deficient NMDAR function that results in a severe deficit in the capacity to induce LTP, with coincident defects in hippocampal-dependent memory (Figure 7E).

DISCUSSION

Many proteins that are essential for normal neural development are also expressed in the adult brain, raising the intriguing possibility that they may in some way influence plasticity. Here, we report that DCC-dependent activation of Src in mature hippocampal neurons is required for the induction of NMDAR-dependent LTP, and that DCC expression by forebrain neurons contributes to spatial and recognition forms of memory. Furthermore, DCC deletion from mature neurons resulted in shorter

Please cite this article in press as: Horn et al., DCC Expression by Neurons Regulates Synaptic Plasticity in the Adult Brain, Cell Reports (2013), http://dx.doi.org/10.1016/j.celrep.2012.12.005

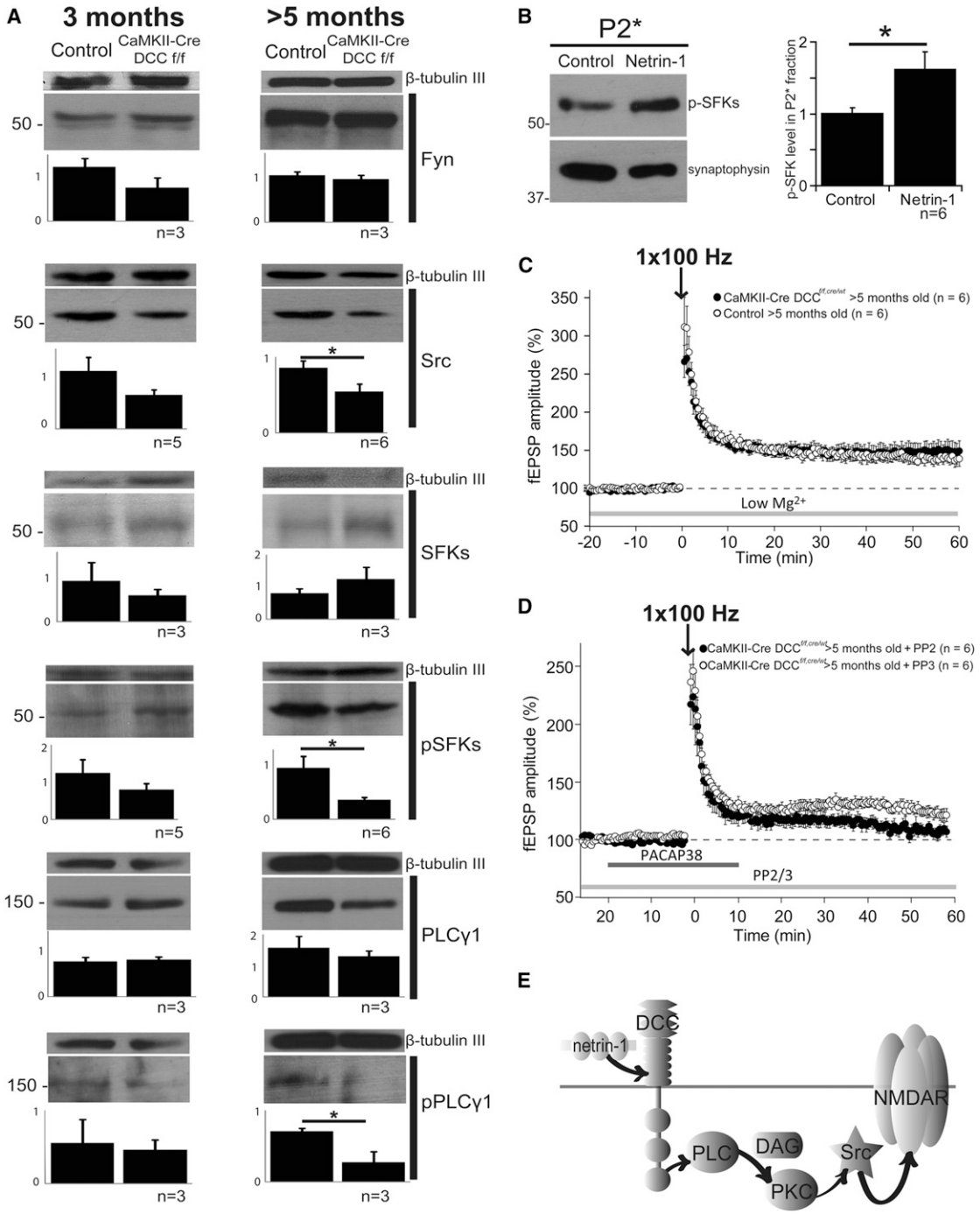

Figure 7. Netrin-1 and DCC Regulate Src Activation

(A) Phosphorylated and total SFKs and PLCγ1 proteins in hippocampal homogenates in control and $DCC^{f/f,cre+}$ mice, normalized to β-tubulin III (n/genotype under histogram; two-tailed t test, *$p < 0.05$). Error bars depict SEM.

(B) Netrin-1 stimulation of P2* purified synaptosomal fraction isolated from adult WT brain significantly increases levels of pSFKs, normalized to synaptophysin as a loading control (n = 6/condition; two-tailed t test, *$p < 0.05$; error bars depict SEM).

(C) Slices from older (>5 months) control and $DCC^{f/f,cre+}$ mice in reduced 1.3 mM Mg^{2+} ACSF remain significantly potentiated 1 hr after HFS (1 s, 100 Hz, 148.6% ± 10.9% in $DCC^{f/f,cre+}$; 139.4% ± 6.6% in age-matched controls; $p < 0.01$).

(D) Slices from older $DCC^{f/f,cre+}$ mice treated with PACAP-38 during HFS and perfused with ACSF containing 2.0 mM Mg^{2+} and the inactive compound PP3 remain significantly potentiated after 1 hr. The SFK inhibitor PP2 blocks potentiation (124.7% ± 4.5% in PP3; 108.2% ± 7.7% in PP2; $p < 0.05$).

(E) Model.

Please cite this article in press as: Horn et al., DCC Expression by Neurons Regulates Synaptic Plasticity in the Adult Brain, Cell Reports (2013), http://dx.doi.org/10.1016/j.celrep.2012.12.005

dendritic spines and increased levels of NMDAR subunit GluN2B, indicating that DCC is required to maintain mature synaptic morphology and an appropriate balance of NMDAR subunit expression. These findings identify a role for DCC as an essential upstream activator of Src signaling at mature CNS synapses, and of synaptic plasticity and memory formation in the mature mammalian brain.

A key aspect of these findings is the relatively minor differences detected between young $DCC^{f/f,cre+}$ and control mice, and the increased severity of the deficits with age, which support the conclusion that impairments develop during aging due to loss of DCC function in neurons. At P14, the level of DCC protein in the hippocampus of $DCC^{f/f,cre+}$ mice did not differ from that in controls. Between P14 and 3 months of age, levels of DCC protein were substantially reduced. Although memory was intact and significant changes in most synapse-associated proteins were not detected in young (2–4 months) $DCC^{f/f,cre+}$ mice, increased levels of GluN2B were present in the hippocampal homogenates of these mice. This indicates that although DCC loss has not yet resulted in dramatic defects, the initial consequences of deleting DCC can be detected at this age. In contrast, levels of Src, pSFK, PLCγ1, and pPLCγ1 in young $DCC^{f/f,cre+}$ mice were not significantly different compared with controls. Mean levels of Src and pSFK showed a tendency to be slightly reduced, however, which may represent the onset of deficits that become more severe in older animals. We conclude that DCC expression by these neurons is essential to maintain the function of synapses that contribute to memory, but that in young adult mice (2–4 months), the deficits are not yet sufficiently severe to disrupt memory formation. These findings support the hypothesis that DCC loss results in a progressive deficit in synapse function as the mice age.

Beyond Axon Guidance: A Postsynaptic Function for DCC in Mature Neurons

Subcellular fractionation and immunohistochemical analyses indicate that DCC is enriched in dendritic spines and associated with the PSD. Previous studies of DCC function in neurons focused on axonal growth cones, where DCC directs the organization of F-actin to regulate motility and adhesion (Lai Wing Sun et al., 2011). Actin is also the major cytoskeletal element that regulates the structure of dendritic filopodia and spines. Notably, the actin regulatory proteins Nck1 (Dock), Pak1, and Rho GTPases (Cdc42, Rac1, and RhoA) all regulate dendritic spine morphology (Tada and Sheng, 2006), and all are downstream effectors of DCC in axons (Lai Wing Sun et al., 2011). Our findings raise the possibility that DCC functions in dendrites upstream of Rho GTPases to maintain mature dendritic spine morphology.

Little, if any, DCC immunoreactivity was detected in presynaptic terminals in mature neurons. This is in contrast to the role of DCC in directing extending axons, which upon reaching an appropriate target form presynaptic terminals. Our findings highlight a postsynaptic role for DCC; however, it remains to be determined how DCC is distributed within dendrites during maturation, when DCC becomes predominantly localized to postsynaptic spines, and whether DCC function in mature neurons is restricted to a postsynaptic role.

DCC Regulation of GluN2B Expression

Following DCC loss, we detected increased levels of the NMDAR subunit GluN2B. During early development, high levels of GluN2B relative to GluN2A are normally present at synapses, with a switch to more GluN2A and less GluN2B occurring during maturation (Barria and Malinow, 2002; Sheng et al., 1994; Williams et al., 1993). NMDARs present at immature hippocampal synapses are largely GluN1-2B complexes (Tovar and Westbrook, 1999) that are thought to inhibit the recruitment of AMPAR GluA1 subunits to the plasma membrane and compromise synapse maturation (Kim et al., 2005). Interestingly, transgenic mice that selectively increase GluN2B expression in forebrain neurons exhibit enhanced hippocampal LTP and improved learning and memory (Tang et al., 1999). In contrast, we found that increased GluN2B expression due to DCC deletion is associated with a deficit in LTP induction and compromised spatial and recognition memory. Importantly, although we detected increased GluN2B protein in hippocampal homogenates and in the LP1 synaptosomal plasma membrane fraction isolated from mature brain, electrophysiological analyses revealed no difference in the contribution of GluN2B to fEPSP responses between genotypes, suggesting that the increased GluN2B detected in $DCC^{f/f,cre+}$ mice may be chiefly extrasynaptic. This suggests that defects induced by loss of DCC may occlude the expected enhancement of synapse function induced by increasing levels of GluN2B.

Netrin-1 and DCC Function at Synapses

The requirement for DCC in activity-dependent plasticity raises questions about how DCC and netrins might be regulated by activity. Both netrin-1 and DCC are enriched in the LP2 fraction of adult brain synaptosomes, consistent with trafficking in cargo vesicles at synapses. Whether netrin-1 is secreted from neurons by constitutive or regulated pathways is unknown, and it remains to be determined whether exocytosis of netrin-1 may be regulated in an activity-dependent manner. In contrast, we previously reported that membrane depolarization recruits DCC to the plasma membrane of embryonic cortical neurons, and that this promotes axon outgrowth in response to netrin-1 (Bouchard et al., 2008). This finding raises the tantalizing possibility that DCC trafficking may be similarly regulated by activity at synapses, and that activity-induced recruitment of DCC to the synaptic plasma membrane may enhance NMDAR function.

Src Is Essential for LTP Induction

Netrin-1 signaling through DCC activates PLCγ (Xie et al., 2006) and Src in neurons (Li et al., 2004), and activation of Src by PLC (MacDonald et al., 2007) is required for Schaffer collateral CA1 NMDAR-dependent LTP (Lu et al., 1998). The NMDAR GluN2A subunit is phosphorylated by Src (Salter and Kalia, 2004), and NMDAR function is enhanced by signaling from PLC to PKC to activate Src (MacDonald et al., 2007). DCC-deficient mice exhibit reduced levels of Src protein, reduced activation of SFK and PLCγ, and a severe deficit in the induction of LTP. We therefore tested the hypothesis that reduced activation of Src results in a deficit in NMDAR function that underlies the absence of LTP. We found that enhancing NMDAR function either by decreasing extracellular levels of Mg^{2+} or by

pharmacologically activating Src completely rescued LTP in $DCC^{f/f,cre+}$ mice. We conclude that DCC expression by hippocampal pyramidal neurons is essential to maintain the morphology of mature dendritic spines, and that DCC activation of Src is required for the induction of NMDAR-dependent LTP, with consequences critical for memory in adult animals.

EXPERIMENTAL PROCEDURES

Animals

All procedures involving animals were performed in accordance with the Canadian Council on Animal Care's guidelines for the use of animals in research. T29-1 CaMKIIα-cre mice were obtained from The Jackson Laboratory (Bar Harbor, ME, USA). Floxed DCC mice were generated as previously described (Krimpenfort et al., 2012).

Immunostaining

Western blot analyses utilized the following antibodies: mouse α-β-tubulin III (1:500, T4026; Sigma-Aldrich, St. Louis, MO, USA), mouse α-DCCin (1:1,000, 554223; BD PharMingen, San Diego, CA, USA), rabbit α-Fyn (gift of Dr. Andre Veillete; Davidson et al., 1992), rabbit α-GluR1 (1:1,000, AB1504; Chemicon, Temecula, CA, USA), rabbit α-GluR2/3 (1:1,000, AB1506; Chemicon), mouse α-NR2B (1:3000, N59/60; NeuroMab, Davis, CA, USA), rabbit α-NSF (1:5,000, AB1764; Chemicon), mouse α-phospho-PLCγ1 (1:200, pY783.27; Santa Cruz Biotechnology, Santa Cruz, CA, USA), rabbit α-phospho-Src family (Tyr416; 1:1,000, 2101; Cell Signaling Technology, Beverly, MA, USA), mouse α-PLCγ1 (1:1,000, 05-163; Millipore, Billerica, MA, USA), mouse α-PSD95 (1:500; BD PharMingen), mouse α-Src family (WTAPE), clone 2E8.2 (1:1,000, 05-1461; Millipore), and mouse α-synaptophysin (1:10,000, S-5768; Sigma-Aldrich).

Immunohistochemical analyses of 16 μm cryostat sections utilized α-β-tubulin III, goat polyclonal α-DCCex (1:500, A20: sc-6535; Santa Cruz Biotechnology), Hoechst stain (1:10,000, 33258; Sigma-Aldrich), and secondary donkey α-goat Alexa-488 (1:500, A11055; Invitrogen, Eugene, OR, USA) or donkey α-mouse Alexa-555 (1:500, A31570; Invitrogen).

Confocal and Electron Microscopy

Axonal-oligodendroglial paranodes labeled with mouse α-Caspr (#75-001; NeuroMab) and rabbit α-Kv1.2 (#APC-010; Alomone Labs, Jerusalem, Israel) were imaged with a confocal microscope (510 LSM; Carl Zeiss, Toronto, Canada). Immunoelectron microscopy on adult rat CA1 followed a pre-embedding immunoperoxidase protocol as previously described (Tremblay et al., 2009) using mouse α-DCCin (1:200, G97-449; BD PharMingen), and sections were examined at 60 kV (CM100 electron microscope; Philips, Eindhoven, The Netherlands).

Subcellular Fractionation

Subcellular fractionation utilized adult rat brain and mouse hippocampi or cortex as previously described (Huttner et al., 1983). PSD fractionation of adult rat brain (unstripped, 7–8 weeks old, ID 56004-2; Pel-Freez Biologicals, Rogers, AR, USA) was carried out as previously described (Fallon et al., 2002). Western blots were probed with antibodies against DCCin, GluR1, netrin-1 (rabbit polyclonal PN2, 11760; Manitt et al., 2001), NR2B, PSD-95, synaptophysin, and synaptotagmin (rabbit polyclonal 8907, provided by P. De Camilli, Yale University, New Haven, CT, USA).

Organotypic Slice Culture and Spine Morphology

Slices (250 μm thick) from the hippocampi of P0 DCC knockout pups and WT littermates were cultured 60 DIV, infected with a virus encoding farnesylated fluorescent protein, and fixed 24 hr later. Analysis of spines (WT: n = 275 spines; $DCC^{-/-}$: n = 392 spines) used Reconstruct software (John Fiala, Boston University, Boston, MA, USA).

Golgi Staining and Spine Morphology

Mouse brains (n = 3/condition) were processed (FD Rapid GolgiStain Kit; FD Neurotechnologies, Catonsville, MD, USA) and ≥50 μm sections were cut with a cryostat. CA1 dendrite segments were traced and analyzed (Neurolucida 9 and NeuroExplorer 9; MBF Bioscience, Williston, VT, USA; spines in young mice: WT: n = 204, $DCC^{f/f,cre+}$: n = 208; spines in aged mice: WT: n = 192, $DCC^{f/f,cre+}$: n = 267; dendritic segments young: WT: n = 11, $DCC^{f/f,cre+}$: n = 11; dendritic segments aged: WT: n = 13, $DCC^{f/f,cre+}$: n = 15).

Morris Water Maze

Mice were trained to find a submerged platform in a water maze in an 8-day training protocol as previously described (Nicolakakis et al., 2011). Swimming was tracked with the use of an overhead video tracking system (2020 Plus tracking system, Ganz FC62D video camera; HVS Image, Mountain View, CA, USA) and tracking software (Water 2020 software; HVS Image). The time and distance traveled in each quadrant were calculated using Water 2020 software.

Novel-Object-Recognition Test

Recognition memory was assessed by means of the novel-object-recognition test (Bevins and Besheer, 2006). Exploration time (duration ≤ body length away from the object, head pointed toward object) was recorded by overhead video (VideoTrack; ViewPoint Life Sciences, Otterburn Park, QC, Canada). Recordings (24 mice/genotype) were assessed by an investigator who was blind to genotype. Difference score = (time with novel object – time with familiar object). Cognition score = (time with novel object/total exploration time).

Electrophysiology

Acute brain slices (350–400 μm) were obtained from mice as previously described (Glasgow and Chapman, 2007, 2008). During recording, slices were continuously perfused with oxygenated ACSF (95% O_2, 5% CO_2, 1.5–2 ml/min).

LTP and LTD tests began after 20–30 min baseline (intensity adjusted to evoke responses 40%–70% of maximum). LTD was assessed with prolonged PPLFS (900 paired pulses, 25 ms interval, 1 Hz for 15 min). LTP was induced by HFS (1 s, 100 Hz train). In the LTP rescue experiment with reduced Mg^{2+}, the ACSF contained 1.3 mM Mg^{2+} and 2.5 mM Ca^{2+} (versus 2 mM Mg^{2+} and 2 mM Ca^{2+}). In the LTP rescue experiment with PACAP-38, either PP2 or PP3 (1 μM in DMSO) was present in the 2.0 mM Mg^{2+} ACSF for the duration of recording, and PACAP-38 (1 nM) was administered from 10 min before HFS to 20 min after HFS. For analysis of fEPSPs in the presence of pharmacological inhibitors, slices were recorded in low-Mg^{2+} ACSF (0.1 mM Mg^{2+}) to which 100 μM PTX, 5 μM CNQX, 3 μM ifenprodil, and 100 μM APV (Tocris, Minneapolis, MN, USA) were added sequentially.

Data Analysis

Statistical significance was tested at the 95% confidence level ($p < 0.05$). In the graphs, error bars indicate SEM. Student's two-tailed t test was used to compare differences between two means.

For additional details, see Extended Experimental Procedures.

SUPPLEMENTAL INFORMATION

Supplemental Information includes Extended Experimental Procedures and can be found with this article online at http://dx.doi.org/10.1016/j.celrep.2012.12.005.

LICENSING INFORMATION

ACKNOWLEDGMENTS

We thank W. Sossin, A. Di Polo, and J. Goldman for critical discussions, and M. Cayouette and D. Bowie for reagents. The project was supported by CIHR operating grant #247564 to T.E.K. K.E.H. was funded by a CIHR Frederick

Banting and Charles Best Canada Graduate Scholarship Doctoral Award. S.D.G. received grants from NSERC, and C.A.C. received grants from NSERC and FRSQ. D.G. holds an FRSQ postdoctoral fellowship. M.E.T. held an FRSQ doctoral training award. E.S.R. holds a tier II Canada Research Chair. T.E.K. holds an FRSQ Chercheur Nationaux award and is a Killam Foundation Scholar.

Received: May 21, 2012
Revised: October 1, 2012
Accepted: December 13, 2012
Published: January 3, 2013

REFERENCES

Barria, A., and Malinow, R. (2002). Subunit-specific NMDA receptor trafficking to synapses. Neuron *35*, 345–353.

Bayer, K.U., Löhler, J., Schulman, H., and Harbers, K. (1999). Developmental expression of the CaM kinase II isoforms: ubiquitous gamma- and delta-CaM kinase II are the early isoforms and most abundant in the developing nervous system. Brain Res. Mol. Brain Res. *70*, 147–154.

Benson, D.L., Isackson, P.J., Gall, C.M., and Jones, E.G. (1992). Contrasting patterns in the localization of glutamic acid decarboxylase and Ca2+/calmodulin protein kinase gene expression in the rat central nervous system. Neuroscience *46*, 825–849.

Bevins, R.A., and Besheer, J. (2006). Object recognition in rats and mice: a one-trial non-matching-to-sample learning task to study 'recognition memory'. Nat. Protoc. *1*, 1306–1311.

Bliss, T.V., and Collingridge, G.L. (1993). A synaptic model of memory: long-term potentiation in the hippocampus. Nature *361*, 31–39.

Bouchard, J.F., Horn, K.E., Stroh, T., and Kennedy, T.E. (2008). Depolarization recruits DCC to the plasma membrane of embryonic cortical neurons and enhances axon extension in response to netrin-1. J. Neurochem. *107*, 398–417.

Burgin, K.E., Waxham, M.N., Rickling, S., Westgate, S.A., Mobley, W.C., and Kelly, P.T. (1990). In situ hybridization histochemistry of Ca2+/calmodulin-dependent protein kinase in developing rat brain. J. Neurosci. *10*, 1788–1798.

Clark, R.E., and Martin, S.J. (2005). Interrogating rodents regarding their object and spatial memory. Curr. Opin. Neurobiol. *15*, 593–598.

Colón-Ramos, D.A., Margeta, M.A., and Shen, K. (2007). Glia promote local synaptogenesis through UNC-6 (netrin) signaling in C. elegans. Science *318*, 103–106.

Davidson, D., Chow, L.M., Fournel, M., and Veillette, A. (1992). Differential regulation of T cell antigen responsiveness by isoforms of the src-related tyrosine protein kinase p59fyn. J. Exp. Med. *175*, 1483–1492.

Fallon, L., Moreau, F., Croft, B.G., Labib, N., Gu, W.J., and Fon, E.A. (2002). Parkin and CASK/LIN-2 associate via a PDZ-mediated interaction and are co-localized in lipid rafts and postsynaptic densities in brain. J. Biol. Chem. *277*, 486–491.

Fazeli, A., Dickinson, S.L., Hermiston, M.L., Tighe, R.V., Steen, R.G., Small, C.G., Stoeckli, E.T., Keino-Masu, K., Masu, M., Rayburn, H., et al. (1997). Phenotype of mice lacking functional Deleted in colorectal cancer (Dcc) gene. Nature *386*, 796–804.

Glasgow, S.D., and Chapman, C.A. (2007). Local generation of theta-frequency EEG activity in the parasubiculum. J. Neurophysiol. *97*, 3868–3879.

Glasgow, S.D., and Chapman, C.A. (2008). Conductances mediating intrinsic theta-frequency membrane potential oscillations in layer II parasubicular neurons. J. Neurophysiol. *100*, 2746–2756.

Haber, M., Zhou, L., and Murai, K.K. (2006). Cooperative astrocyte and dendritic spine dynamics at hippocampal excitatory synapses. J. Neurosci. *26*, 8881–8891.

Huttner, W.B., Schiebler, W., Greengard, P., and De Camilli, P. (1983). Synapsin I (protein I), a nerve terminal-specific phosphoprotein. III. Its association with synaptic vesicles studied in a highly purified synaptic vesicle preparation. J. Cell Biol. *96*, 1374–1388.

Jacobs, K.M., Neve, R.L., and Donoghue, J.P. (1993). Neocortex and hippocampus contain distinct distributions of calcium-calmodulin protein kinase II and GAP43 mRNA. J. Comp. Neurol. *336*, 151–160.

Jarjour, A.A., Bull, S.J., Almasieh, M., Rajasekharan, S., Baker, K.A., Mui, J., Antel, J.P., Di Polo, A., and Kennedy, T.E. (2008). Maintenance of axo-oligodendroglial paranodal junctions requires DCC and netrin-1. J. Neurosci. *28*, 11003–11014.

Kim, M.J., Dunah, A.W., Wang, Y.T., and Sheng, M. (2005). Differential roles of NR2A- and NR2B-containing NMDA receptors in Ras-ERK signaling and AMPA receptor trafficking. Neuron *46*, 745–760.

Kolodziej, P.A., Timpe, L.C., Mitchell, K.J., Fried, S.R., Goodman, C.S., Jan, L.Y., and Jan, Y.N. (1996). frazzled encodes a Drosophila member of the DCC immunoglobulin subfamily and is required for CNS and motor axon guidance. Cell *87*, 197–204.

Kourrich, S., Glasgow, S.D., Caruana, D.A., and Chapman, C.A. (2008). Postsynaptic signals mediating induction of long-term synaptic depression in the entorhinal cortex. Neural Plast. *2008*, 840374.

Krimpenfort, P., Song, J.Y., Proost, N., Zevenhoven, J., Jonkers, J., and Berns, A. (2012). Deleted in colorectal carcinoma suppresses metastasis in p53-deficient mammary tumours. Nature *482*, 538–541.

Lai Wing Sun, K., Correia, J.P., and Kennedy, T.E. (2011). Netrins: versatile extracellular cues with diverse functions. Development *138*, 2153–2169.

Li, W., Lee, J., Vikis, H.G., Lee, S.H., Liu, G., Aurandt, J., Shen, T.L., Fearon, E.R., Guan, J.L., Han, M., et al. (2004). Activation of FAK and Src are receptor-proximal events required for netrin signaling. Nat. Neurosci. *7*, 1213–1221.

Liu, G., Beggs, H., Jürgensen, C., Park, H.T., Tang, H., Gorski, J., Jones, K.R., Reichardt, L.F., Wu, J., and Rao, Y. (2004). Netrin requires focal adhesion kinase and Src family kinases for axon outgrowth and attraction. Nat. Neurosci. *7*, 1222–1232.

Livesey, F.J., and Hunt, S.P. (1997). Netrin and netrin receptor expression in the embryonic mammalian nervous system suggests roles in retinal, striatal, nigral, and cerebellar development. Mol. Cell. Neurosci. *8*, 417–429.

Lu, Y.M., Roder, J.C., Davidow, J., and Salter, M.W. (1998). Src activation in the induction of long-term potentiation in CA1 hippocampal neurons. Science *279*, 1363–1367.

Macdonald, D.S., Weerapura, M., Beazely, M.A., Martin, L., Czerwinski, W., Roder, J.C., Orser, B.A., and MacDonald, J.F. (2005). Modulation of NMDA receptors by pituitary adenylate cyclase activating peptide in CA1 neurons requires G alpha q, protein kinase C, and activation of Src. J. Neurosci. *25*, 11374–11384.

MacDonald, J.F., Jackson, M.F., and Beazely, M.A. (2007). G protein-coupled receptors control NMDARs and metaplasticity in the hippocampus. Biochim. Biophys. Acta *1768*, 941–951.

Manitt, C., Colicos, M.A., Thompson, K.M., Rousselle, E., Peterson, A.C., and Kennedy, T.E. (2001). Widespread expression of netrin-1 by neurons and oligodendrocytes in the adult mammalian spinal cord. J. Neurosci. *21*, 3911–3922.

Manitt, C., Nikolakopoulou, A.M., Almario, D.R., Nguyen, S.A., and Cohen-Cory, S. (2009). Netrin participates in the development of retinotectal synaptic connectivity by modulating axon arborization and synapse formation in the developing brain. J. Neurosci. *29*, 11065–11077.

Mitchell, K.J., Doyle, J.L., Serafini, T., Kennedy, T.E., Tessier-Lavigne, M., Goodman, C.S., and Dickson, B.J. (1996). Genetic analysis of Netrin genes in Drosophila: Netrins guide CNS commissural axons and peripheral motor axons. Neuron *17*, 203–215.

Miyata, A., Jiang, L., Dahl, R.D., Kitada, C., Kubo, K., Fujino, M., Minamino, N., and Arimura, A. (1990). Isolation of a neuropeptide corresponding to the N-terminal 27 residues of the pituitary adenylate cyclase activating polypeptide with 38 residues (PACAP38). Biochem. Biophys. Res. Commun. *170*, 643–648.

Nicolakakis, N., Aboulkassim, T., Aliaga, A., Tong, X.K., Rosa-Neto, P., and Hamel, E. (2011). Intact memory in TGF-beta1 transgenic mice featuring

chronic cerebrovascular deficit: recovery with pioglitazone. J. Cereb. Blood Flow Metab. *31*, 200–211.

Nimchinsky, E.A., Sabatini, B.L., and Svoboda, K. (2002). Structure and function of dendritic spines. Annu. Rev. Physiol. *64*, 313–353.

Poon, V.Y., Klassen, M.P., and Shen, K. (2008). UNC-6/netrin and its receptor UNC-5 locally exclude presynaptic components from dendrites. Nature *455*, 669–673.

Salter, M.W., and Kalia, L.V. (2004). Src kinases: a hub for NMDA receptor regulation. Nat. Rev. Neurosci. *5*, 317–328.

Sauer, B. (1998). Inducible gene targeting in mice using the Cre/lox system. Methods *14*, 381–392.

Serafini, T., Colamarino, S.A., Leonardo, E.D., Wang, H., Beddington, R., Skarnes, W.C., and Tessier-Lavigne, M. (1996). Netrin-1 is required for commissural axon guidance in the developing vertebrate nervous system. Cell *87*, 1001–1014.

Shen, K., and Cowan, C.W. (2010). Guidance molecules in synapse formation and plasticity. Cold Spring Harb. Perspect. Biol. *2*, a001842.

Sheng, M., Cummings, J., Roldan, L.A., Jan, Y.N., and Jan, L.Y. (1994). Changing subunit composition of heteromeric NMDA receptors during development of rat cortex. Nature *368*, 144–147.

Sonner, J.M., Cascio, M., Xing, Y., Fanselow, M.S., Kralic, J.E., Morrow, A.L., Korpi, E.R., Hardy, S., Sloat, B., Eger, E.I., 2nd, and Homanics, G.E. (2005). Alpha 1 subunit-containing GABA type A receptors in forebrain contribute to the effect of inhaled anesthetics on conditioned fear. Mol. Pharmacol. *68*, 61–68.

Soriano, P. (1999). Generalized lacZ expression with the ROSA26 Cre reporter strain. Nat. Genet. *21*, 70–71.

Stavoe, A.K., and Colón-Ramos, D.A. (2012). Netrin instructs synaptic vesicle clustering through Rac GTPase, MIG-10, and the actin cytoskeleton. J. Cell Biol. *197*, 75–88.

Tada, T., and Sheng, M. (2006). Molecular mechanisms of dendritic spine morphogenesis. Curr. Opin. Neurobiol. *16*, 95–101.

Tang, Y.P., Shimizu, E., Dube, G.R., Rampon, C., Kerchner, G.A., Zhuo, M., Liu, G., and Tsien, J.Z. (1999). Genetic enhancement of learning and memory in mice. Nature *401*, 63–69.

Tovar, K.R., and Westbrook, G.L. (1999). The incorporation of NMDA receptors with a distinct subunit composition at nascent hippocampal synapses in vitro. J. Neurosci. *19*, 4180–4188.

Tremblay, M.E., Riad, M., Chierzi, S., Murai, K.K., Pasquale, E.B., and Doucet, G. (2009). Developmental course of EphA4 cellular and subcellular localization in the postnatal rat hippocampus. J. Comp. Neurol. *512*, 798–813.

Tsien, J.Z., Chen, D.F., Gerber, D., Tom, C., Mercer, E.H., Anderson, D.J., Mayford, M., Kandel, E.R., and Tonegawa, S. (1996). Subregion- and cell type-restricted gene knockout in mouse brain. Cell *87*, 1317–1326.

Volenec, A., Bhogal, R.K., Moorman, J.M., Leslie, R.A., and Flanigan, T.P. (1997). Differential expression of DCC mRNA in adult rat forebrain. Neuroreport *8*, 2913–2917.

Williams, K., Russell, S.L., Shen, Y.M., and Molinoff, P.B. (1993). Developmental switch in the expression of NMDA receptors occurs in vivo and in vitro. Neuron *10*, 267–278.

Winberg, M.L., Mitchell, K.J., and Goodman, C.S. (1998). Genetic analysis of the mechanisms controlling target selection: complementary and combinatorial functions of netrins, semaphorins, and IgCAMs. Cell *93*, 581–591.

Xie, Y., Hong, Y., Ma, X.Y., Ren, X.R., Ackerman, S., Mei, L., and Xiong, W.C. (2006). DCC-dependent phospholipase C signaling in netrin-1-induced neurite elongation. J. Biol. Chem. *281*, 2605–2611.

Yu, X.M., and Salter, M.W. (1998). Gain control of NMDA-receptor currents by intracellular sodium. Nature *396*, 469–474.

Yu, X.M., Askalan, R., Keil, G.J., 2nd, and Salter, M.W. (1997). NMDA channel regulation by channel-associated protein tyrosine kinase Src. Science *275*, 674–678.

Zhou, C.J., Kikuyama, S., Shibanuma, M., Hirabayashi, T., Nakajo, S., Arimura, A., and Shioda, S. (2000). Cellular distribution of the splice variants of the receptor for pituitary adenylate cyclase-activating polypeptide (PAC(1)-R) in the rat brain by in situ RT-PCR. Brain Res. Mol. Brain Res. *75*, 150–158.